IEEE Access
Multidisciplinary | Rapid Review | Open Access Journal

Received July 9, 2019, accepted July 17, 2019, date of publication July 22, 2019, date of current version August 12, 2019.

Digital Object Identifier 10.1109/ACCESS.2019.2930323

Neural Dynamics for Control of Industrial Agitator Tank With Rapid Convergence and Perturbations Rejection

WENHUI DUAN[1,4], XIUCHUN XIAO[2], DONGYANG FU[2], JINGWEN YAN[3], MEI LIU[1], JILIANG ZHANG[1], (Member, IEEE), AND LONG JIN[1,4], (Member, IEEE)

[1]School of Information Science and Engineering, Lanzhou University, Lanzhou 730000, China
[2]College of Electronic and Information Engineering, Guangdong Ocean University, Zhanjiang 524088, China
[3]College of Engineering, Shantou University, Shantou 515063, China
[4]State Key Laboratory of Management and Control for Complex Systems, Institute of Automation, Chinese Academy of Sciences, Beijing 100190, China

Corresponding authors: Xiuchun Xiao (xcxiao@hotmail.com) and Jingwen Yan (jwyan@stu.edu.cn)

This work was supported in part by the National Natural Science Foundation of China under Grant 61703189, in part by the International Science and Technology Cooperation Program of China under Grant 2017YFE0118900, in part by the Key Laboratory of Digital Signal and Image Processing of Guangdong Province under Grant 2016GDDSIPL-02, in part by the Doctoral Initiating Project of Guangdong Ocean University under Grant E13428, in part by the Innovation and Strength Project of Guangdong Ocean University under Grant Q15090 and Grant 230419065, in part by the Natural Science Foundation of Gansu Province, China, under Grant 18JR3RA264, in part by the Sichuan Science and Technology Program under Grant 19YYJC1656, in part by the State Key Laboratory of Management and Control for Complex Systems, Institute of Automation, Chinese Academy of Sciences under Grant 20190112, and in part by the Fundamental Research Funds for the Central Universities under Grant lzujbky-2019-89.

ABSTRACT The industrial agitator tank is a widely used equipment in the chemical industry for the production of the chemical reagents. The high-performance agitator tank controller is critical to increase its productivity. In this paper, we propose an agitator tank controller based on a neural dynamics method with a shorter error-converging time in comparison with the existing methods. In addition, the controller also has a strong capability to reject perturbations. Furthermore, the superiority of the proposed agitator tank controller is theoretically analyzed. Ultimately, computer simulations synthesized by the proposed agitator tank controller are conducted. The numerical results validate the superior performance of the proposed controller.

INDEX TERMS Chemical industry, automatic control, control design, neural dynamics method, rapid convergence, perturbations rejection.

I. INTRODUCTION

Chemical industry is indispensable to heavy industry, to a large extent [1], [2]. The chemical industry mainly produces chemical products [3], [4], such as chemical reagents, biological reagents and farm chemicals [5], [6]. Industrial agitator tanks are frequently used to the production of these reagents. Therefore, the agitator tank performs a crucial role in the chemical industry [7], [8]. As the step of science and technology development accelerates, the variety and function of chemical reagents are increasing abundantly [9], [10]. As a typical nonlinear system, the agitator tank has received extensive attention from researchers in order to develop a high-performance agitator tank controller [11]–[17].

The rapid development of artificial intelligence has attracted the wide attention of researchers in recent years. As a significant subtopic of machine learning, neural networks are widely used in various spheres [18]–[32]. In the field of control systems for agitator tanks, many control methods have been presented [33], [34]. For example, Cai et al. designed a dry mortar mixing storage control system on the basis of the backward propagation (BP) neural proportional-integral-derivative (PID) controller [33]. The system can solve the control problem of complex dynamic systems by correcting the weight coefficient of the neural network in the control process according to the gradient descent method. Moreover, Zhang et al. first presented a controller of agitator tank based on Taylor finite difference [34]. The controller is an error-based dynamic method, which can make the error function converge to zero. The agitator tank equipped with the controller is able to prepare the reagent of desired concentration quickly. Nevertheless, the controller does not consider that the agitator tank may be disturbed during the actual operation. Note that the agitator tank may be disturbed

The associate editor coordinating the review of this manuscript and approving it for publication was Chaoyong Li.

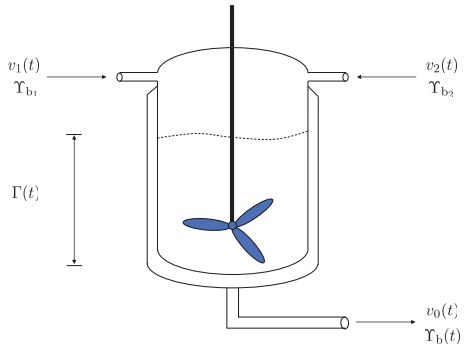

FIGURE 1. The schematic of traditional industrial agitator tank equipment.

in a practical manufacturing scenario during operation. The interference could lead to inaccuracy of the reagent concentration, and lead to a waste of materials. Consequently, the existing agitator tank control methods have the above mentioned defects [33]–[44].

To compensate for these defects of the existing agitator tank controllers, a new controller based on the neural dynamics method is proposed in this paper [45]–[47]. The proposed controller enables the concentration of the output solution of the agitator tank to quickly converge to the desired one. Therefore, the controller has perturbations rejection performance. As an evolution beyond existing methods, the proposed controller ensures that the system of the agitator tank can effectively eliminate perturbations. This advantage of perturbations rejection is of great significance for improving the performance of the existing agitator tank. As a result, the agitator tank equipped with the proposed controller continuously outputs the solution of the target concentration.

The remainder of this paper is organized as follows. Section II describes the dynamic equation of the agitator tank system and gives the system parameters. The design steps of the agitator tank controller are presented in Section III. In addition, Section IV demonstrates the rapid convergence performance and perturbations rejection performance of the agitator tank from the theoretical perspective. Simulation results are presented in Section V to show the superior performance of the proposed controller. Section VI concludes this paper. At the end of this section, the main contributions of this paper are summarized as follows.

- In this paper, a new controller of agitator tank is proposed based on the neural dynamics method. Compared with the existing ones, the proposed controller has remarkable advantages.
- The fast convergence rate and the perturbations rejection performance of the proposed controller are analyzed theoretically.
- Computer simulations based on the agitator tanks equipped with different controllers are conducted and comparison results verify the superiority of the proposed controller.

II. DYNAMIC SYSTEM OF THE AGITATOR TANK

In this section, the dynamic system equations of agitator tank are described, which lay the foundation for devising the new controller.

The schematic of traditional industrial agitator tank equipment commonly used in the industrial field is depicted in Fig. 1 with illustrative parameters. As far as the parameters are concerned, Υ_{b1}, Υ_{b2} and Υ_b denote the concentrations of the influent liquids and effluent liquid, respectively; v_1, v_2 and v_0 stand for the flow rates of the influent liquids and effluent liquid, respectively; Γ denotes the liquid volume of the agitator tank. The concentrations of the two influent liquids are unequal for the most part without special claims. Research targets of the agitator tank in this paper are that the concentration of actual solution in the tank can quickly reach the desired value, and that the error of the concentration of solutions can converge to zero with external perturbations.

The system equations of the agitator tank are presented as follows [34]:

$$\dot{\Gamma}(t) = v_1(t) + v_2(t) - 0.2\sqrt{\Gamma(t)}, \tag{1}$$

$$\dot{\Upsilon}_b(t) = \big(\Upsilon_{b1} - \Upsilon_b(t)\big)\frac{v_1(t)}{\Gamma(t)} + \big(\Upsilon_{b2} - \Upsilon_b(t)\big)\frac{v_2(t)}{\Gamma(t)} - \frac{n_1\Upsilon_b(t)}{(1+n_2\Upsilon_b(t))^2}, \tag{2}$$

where t denotes time; $\dot{\Upsilon}_b(t)$ is the time derivative of $\Upsilon_b(t)$; $\dot{\Gamma}(t)$ is the time derivative of $\Gamma(t)$; the outflow rate constants in the dynamic process of the system are denoted by n_1 and n_2.

III. DESIGN STEPS OF THE AGITATOR TANK CONTROLLER

The agitator tank controller is designed and given in this section. First of all, a neural dynamics method is introduced here. Specifically, the residual error function is defined to start the derivation from the viewpoint of control as follows:

$$\epsilon(t) = q(t) - q_d(t), \tag{3}$$

where $q(t)$ represents the actual value and $q_d(t)$ denotes the expected value. When $\epsilon(t)$ converges to zero, the actual value $q(t)$ is approximately equal to the expected one $q_d(t)$. Inspired by the neural dynamics design equation $\dot{\epsilon}(t) = -c\epsilon(t)$ introduced in [34], where $\dot{\epsilon}(t)$ represents the first derivative of $\epsilon(t)$, and $c > 0$ is the scaling factor related to the convergence rate of the residual error, it is modified in [48]–[53] that

$$\dot{\epsilon}(t) = -cP_1\big(\epsilon(t)\big) - dP_2\left\{\epsilon(t) + c\int_0^t P_1\epsilon(\tau)\mathrm{d}\tau\right\}, \tag{4}$$

where the convergence rate parameters of the residual error are denoted by c and $d > 0$; $P_1(\cdot)$ and $P_2(\cdot)$ stand for the monotonically-increasing odd function. Combining (3) and (4) obtains

$$\dot{\epsilon}(t) = -cP_1\big(q(t) - q_d(t)\big) - dP_2\left\{\big(q(t) - q_d(t)\big) + c\int_0^t P_1\big(q(\tau) - q_d(\tau)\big)\mathrm{d}\tau\right\}.$$

The time derivatives of $q(t)$ and $q_{\mathrm{d}}(t)$ are denoted by $\dot{q}(t)$ and $\dot{q_{\mathrm{d}}}(t)$, respectively. Then, according to the parameters of the agitator tank system, the residual error function (3) is expanded as follows:

$$\epsilon_{\Gamma}(t) = \Gamma(t) - \Gamma_{\mathrm{d}}(t), \tag{5}$$

$$\epsilon_{\Upsilon_{\mathrm{b}}}(t) = \Upsilon_{\mathrm{b}}(t) - \Upsilon_{\mathrm{bd}}(t), \tag{6}$$

where $\epsilon_{\Gamma}(t)$ and $\epsilon_{\Upsilon_{\mathrm{b}}}(t)$ stand for the residual error of $\Gamma(t)$ and $\Upsilon_{\mathrm{b}}(t)$, separately; $\Gamma_{\mathrm{d}}(t)$ represents the desired liquid volume of the agitator tank; $\Upsilon_{\mathrm{bd}}(t)$ denotes the desired concentration of the effluent liquid. Calculating the time derivative of $\epsilon_{\Gamma}(t)$ and $\epsilon_{\Upsilon_{\mathrm{b}}}(t)$ obtains

$$\begin{aligned}
&\dot{\epsilon}_{\Gamma}(t)\\
&= \dot{\Gamma}(t) - \dot{\Gamma}_{\mathrm{d}}(t)\\
&= -cP_1\big(\Gamma(t)-\Gamma_{\mathrm{d}}(t)\big)\\
&\quad -dP_2\left\{\big(\Gamma(t)-\Gamma_{\mathrm{d}}(t)\big)+c\int_0^t P_1\big(\Gamma(\tau)-\Gamma_{\mathrm{d}}(\tau)\big)\mathrm{d}\tau\right\},
\end{aligned} \tag{7}$$

$$\begin{aligned}
&\dot{\epsilon}_{\Upsilon_{\mathrm{b}}}(t)\\
&= \dot{\Upsilon}_{\mathrm{b}}(t) - \dot{\Upsilon}_{\mathrm{bd}}(t)\\
&= -cP_1\big(\Upsilon_{\mathrm{b}}(t) - \Upsilon_{\mathrm{bd}}(t)\big)\\
&\quad -dP_2\left\{\big(\Upsilon_{\mathrm{b}}(t)-\Upsilon_{\mathrm{bd}}(t)\big)+c\int_0^t P_1\big(\Upsilon_{\mathrm{b}}(\tau)-\Upsilon_{\mathrm{bd}}(\tau)\big)\mathrm{d}\tau\right\},
\end{aligned} \tag{8}$$

where $\dot{\Gamma}_{\mathrm{d}}(t)$ and $\dot{\Upsilon}_{\mathrm{bd}}(t)$ denote the time derivatives of Γ_{d} and $\Upsilon_{\mathrm{bd}}(t)$, respectively. Combining (7)-(8) and (1)-(2) gets

$$\begin{aligned}
&v_1(t)+v_2(t) - 0.2\sqrt{\Gamma(t)}-\dot{\Gamma}_{\mathrm{d}}(t)\\
&= -cP_1\big(\Gamma(t)-\Gamma_{\mathrm{d}}(t)\big)\\
&\quad -dP_2\left\{\big(\Gamma(t)-\Gamma_{\mathrm{d}}(t)\big)+c\int_0^t P_1\big(\Gamma(\tau)-\Gamma_{\mathrm{d}}(\tau)\big)\mathrm{d}\tau\right\},
\end{aligned} \tag{9}$$

and

$$\begin{aligned}
&\big(\Upsilon_{\mathrm{b1}} - \Upsilon_{\mathrm{b}}(t)\big)\frac{v_1(t)}{\Gamma(t)} + \big(\Upsilon_{\mathrm{b2}} - \Upsilon_{\mathrm{b}}(t)\big)\frac{v_2(t)}{\Gamma(t)}\\
&\quad -\frac{n_1\Upsilon_{\mathrm{b}}(t)}{\big(1+n_2\Upsilon_{\mathrm{b}}(t)\big)^2} - \dot{\Upsilon}_{\mathrm{bd}}(t)\\
&= -cP_1\big(\Upsilon_{\mathrm{b}}(t) - \Upsilon_{\mathrm{bd}}(t)\big)\\
&\quad -dP_2\left\{\big(\Upsilon_{\mathrm{b}}(t)-\Upsilon_{\mathrm{bd}}(t)\big)+c\int_0^t P_1\big(\Upsilon_{\mathrm{b}}(\tau)-\Upsilon_{\mathrm{bd}}(\tau)\big)\mathrm{d}\tau\right\}.
\end{aligned} \tag{10}$$

Finally, after solving (9) and (10), we can get

$$\begin{aligned}
&v_1(t)\\
&= \frac{1}{\big(\Upsilon_{\mathrm{b}_1}-\Upsilon_{\mathrm{b}}(t)\big)}\left\{\frac{n_1\Upsilon_{\mathrm{b}}(t)\Gamma(t)}{\big(1+n_2\Upsilon_{\mathrm{b}}(t)\big)^2}+\dot{\Upsilon}_{\mathrm{bd}}(t)\Gamma(t)\right.\\
&\quad -cP_1\big(\Gamma(t) - \Gamma_{\mathrm{d}}(t)\big)-\big(\Upsilon_{\mathrm{b}_2}-\Upsilon_{\mathrm{b}}(t)\big)v_2(t)\\
&\quad \left.-dP_2\left\{\big(\Gamma(t)-\Gamma_{\mathrm{d}}(t)\big)+c\int_0^t P_1\big(\Gamma(\tau)-\Gamma_{\mathrm{d}}(\tau)\big)\mathrm{d}\tau\right\}\right\},
\end{aligned} \tag{11}$$

$$\begin{aligned}
&v_2(t)\\
&= \frac{1}{\big(\Upsilon_{\mathrm{b}_2}-\Upsilon_{\mathrm{b}}(t)\big)}\left\{\frac{n_1\Upsilon_{\mathrm{b}}(t)\Gamma(t)}{\big(1+n_2\Upsilon_{\mathrm{b}}(t)\big)^2}+\dot{\Upsilon}_{\mathrm{bd}}(t)\Gamma(t)\right.\\
&\quad -cP_1\big(\Upsilon_{\mathrm{b}}(t)-\Upsilon_{\mathrm{bd}}(t)\big)-\big(\Upsilon_{\mathrm{b}_1}-\Upsilon_{\mathrm{b}}(t)\big)v_1(t)\\
&\quad \left.-dP_2\left\{\big(\Upsilon_{\mathrm{b}}(t)-\Upsilon_{\mathrm{bd}}(t)\big)+c\int_0^t P_1\big(\Upsilon_{\mathrm{b}}(\tau)-\Upsilon_{\mathrm{bd}}(\tau)\big)\mathrm{d}\tau\right\}\right\}.
\end{aligned} \tag{12}$$

Simplifying the above two equations obtains the proposed controller:

$$\begin{aligned}
&v_1(t)\\
&= \left\{\left\{0.2\sqrt{\Gamma(t)}+\dot{\Gamma}_{\mathrm{d}}(t) - cP_1\big(\Gamma(t)-\Gamma_{\mathrm{d}}(t)\big)\right.\right.\\
&\quad \left.-dP_2\left\{\big(\Gamma(t)-\Gamma_{\mathrm{d}}(t)\big)+c\int_0^t P_1\big(\Gamma(\tau)-\Gamma_{\mathrm{d}}(\tau)\big)\mathrm{d}\tau\right\}\right\}\\
&\quad \times\big(\Upsilon_{\mathrm{b}_1}-\Upsilon_{\mathrm{b}}(t)\big) - \frac{n_1\Upsilon_{\mathrm{b}}(t)\Gamma(t)}{\big(1+n_2\Upsilon_{\mathrm{b}}(t)\big)^2}-\dot{\Upsilon}_{\mathrm{bd}}(t)\Gamma(t)\\
&\quad \left.+dP_2\left\{\big(\Upsilon_{\mathrm{b}}(t)-\Upsilon_{\mathrm{bd}}(t)\big)+c\int_0^t P_1\big(\Upsilon_{\mathrm{b}}(\tau)-\Upsilon_{\mathrm{bd}}(\tau)\big)\mathrm{d}\tau\right\}\right\}\\
&\quad \times\frac{1}{(\Upsilon_{\mathrm{b}_1}-\Upsilon_{\mathrm{b}_2})} + cP_1\big(\Upsilon_{\mathrm{b}}(t)-\Upsilon_{\mathrm{bd}}(t)\big),
\end{aligned} \tag{13}$$

$$\begin{aligned}
&v_2(t)\\
&= \left\{\left\{0.2\sqrt{\Gamma(t)} + \dot{\Gamma}_{\mathrm{d}}(t) - cP_1\big(\Gamma(t) - \Gamma_{\mathrm{d}}(t)\big)\right.\right.\\
&\quad \left.-dP_2\left\{\big(\Gamma(t)-\Gamma_{\mathrm{d}}(t)\big) + c\int_0^t P_1\big(\Gamma(\tau)-\Gamma_{\mathrm{d}}(\tau)\big)\mathrm{d}\tau\right\}\right\}\\
&\quad \times\big(\Upsilon_{\mathrm{b}_2} - \Upsilon_{\mathrm{b}}(t)\big) - \frac{n_1\Upsilon_{\mathrm{b}}(t)\Gamma(t)}{\big(1+n_2\Upsilon_{\mathrm{b}}(t)\big)^2} - \dot{\Upsilon}_{\mathrm{bd}}(t)\Gamma(t)\\
&\quad \left.+dP_2\left\{\big(\Upsilon_{\mathrm{b}}(t)-\Upsilon_{\mathrm{bd}}(t)\big)+c\int_0^t P_1\big(\Upsilon_{\mathrm{b}}(\tau)-\Upsilon_{\mathrm{bd}}(\tau)\big)\mathrm{d}\tau\right\}\right\}\\
&\quad \times\frac{1}{(\Upsilon_{\mathrm{b}_2}-\Upsilon_{\mathrm{b}_1})}+cP_1\big(\Upsilon_{\mathrm{b}}(t)-\Upsilon_{\mathrm{bd}}(t)\big).
\end{aligned} \tag{14}$$

Further, given that in the actual operation, the agitator tank may be disturbed by external perturbations. We add the interference amount in equation (1) and equation (2) of the agitator tank system. Thus, it has

$$\begin{aligned}
&v_1(t)+M_1(t)+v_2(t)+M_2(t) - 0.2\sqrt{\Gamma(t)}-\dot{\Gamma}_{\mathrm{d}}(t)\\
&\quad -cP_1\big(\Gamma(t)-\Gamma_{\mathrm{d}}(t)\big)\\
&\quad -dP_2\left\{\big(\Gamma(t)-\Gamma_{\mathrm{d}}(t)\big)+c\int_0^t P_1\big(\Gamma(\tau)-\Gamma_{\mathrm{d}}(\tau)\big)\mathrm{d}\tau\right\},
\end{aligned} \tag{15}$$

$$\begin{aligned}
&\big(\Upsilon_{\mathrm{b1}}-\Upsilon_{\mathrm{b}}(t)\big)\frac{v_1(t)+M_1(t)}{\Gamma(t)} + \big(\Upsilon_{\mathrm{b2}} - \Upsilon_{\mathrm{b}}(t)\big)\frac{v_2(t)+M_2(t)}{\Gamma(t)}\\
&\quad -\frac{n_1\Upsilon_{\mathrm{b}}(t)}{\big(1+n_2\Upsilon_{\mathrm{b}}(t)\big)^2} - \dot{\Upsilon}_{\mathrm{bd}}(t) = -cP_1\big(\Upsilon_{\mathrm{b}}(t) - \Upsilon_{\mathrm{bd}}(t)\big)\\
&\quad -dP_2\left\{\big(\Upsilon_{\mathrm{b}}(t)-\Upsilon_{\mathrm{bd}}(t)\big)+c\int_0^t P_1\big(\Upsilon_{\mathrm{b}}(\tau)-\Upsilon_{\mathrm{bd}}(\tau)\big)\mathrm{d}\tau\right\},
\end{aligned} \tag{16}$$

where M_1 and M_2 stand for perturbations. Furthermore, we have

$$\begin{aligned}
&v_1(t)+v_2(t)-0.2\sqrt{\Gamma(t)}-\dot{\Gamma}_{\mathrm{d}}(t)\\
&\quad=-cP_1\big(\Gamma(t)-\Gamma_{\mathrm{d}}(t)\big)\\
&\qquad-dP_2\left\{\big(\Gamma(t)-\Gamma_{\mathrm{d}}(t)\big)+c\int_0^t P_1\big(\Gamma(\tau)-\Gamma_{\mathrm{d}}(\tau)\big)\mathrm{d}\tau\right\}\\
&\qquad-M_1(t)-M_2(t), \qquad (17)\\
&\big(\Upsilon_{\mathrm{b1}}-\Upsilon_{\mathrm{b}}(t)\big)\frac{v_1(t)}{\Gamma(t)}+\big(\Upsilon_{\mathrm{b2}}-\Upsilon_{\mathrm{b}}(t)\big)\frac{v_2(t)}{\Gamma(t)}\\
&\qquad-\frac{n_1\Upsilon_{\mathrm{b}}(t)}{\big(1+n_2\Upsilon_{\mathrm{b}}(t)\big)^2}-\dot{\Upsilon}_{\mathrm{bd}}(t)\\
&\quad=-dP_2\left\{\big(\Upsilon_{\mathrm{b}}(t)-\Upsilon_{\mathrm{bd}}(t)\big)+c\int_0^t P_1\big(\Upsilon_{\mathrm{b}}(\tau)-\Upsilon_{\mathrm{bd}}(\tau)\big)\mathrm{d}\tau\right\}\\
&\qquad-\big(\Upsilon_{\mathrm{b1}}-\Upsilon_{\mathrm{b}}(t)\big)\frac{M_1(t)}{\Gamma(t)}-\big(\Upsilon_{\mathrm{b2}}-\Upsilon_{\mathrm{b}}(t)\big)\frac{M_2(t)}{\Gamma(t)}\\
&\qquad-cP_1\big(\Upsilon_{\mathrm{b}}(t)-\Upsilon_{\mathrm{bd}}(t)\big). \qquad (18)
\end{aligned}$$

Combining formulas (1), (2), (5), (6), (7), and (8), we get

$$\begin{aligned}
&\dot{\epsilon}_{\Gamma}(t)\\
&\quad=-cP_1\big(\Gamma(t)-\Gamma_{\mathrm{d}}(t)\big)+\Psi_{\Gamma}(t)\\
&\qquad-dP_2\left\{\big(\Gamma(t)-\Gamma_{\mathrm{d}}(t)\big)+c\int_0^t P_1\big(\Gamma(\tau)-\Gamma_{\mathrm{d}}(\tau)\big)\mathrm{d}\tau\right\}, \qquad (19)\\
&\dot{\epsilon}_{\Upsilon_{\mathrm{b}}}(t)\\
&\quad=-cP_1\big(\Upsilon_{\mathrm{b}}(t)-\Upsilon_{\mathrm{bd}}(t)\big)+\Psi_{\Upsilon_b}(t)\\
&\qquad-dP_2\left\{\big(\Upsilon_{\mathrm{b}}(t)-\Upsilon_{\mathrm{bd}}(t)\big)+c\int_0^t P_1\big(\Upsilon_{\mathrm{b}}(\tau)-\Upsilon_{\mathrm{bd}}(\tau)\big)\mathrm{d}\tau\right\}, \qquad (20)
\end{aligned}$$

with $\Psi_{\Gamma}(t)=-M_1(t)-M_2(t)$, and $\Psi_{\Upsilon_b}(t)=-\big(\Upsilon_{\mathrm{b1}}-\Upsilon_{\mathrm{b}}(t)\big)M_1(t)/\Gamma(t)-\big(\Upsilon_{\mathrm{b2}}-\Upsilon_{\mathrm{b}}(t)\big)M_2(t)/\Gamma(t)$. At the end of this section, the existing controller in [34] as follows is employed to provide a benchmark for comparison.

$$\begin{aligned}
v_1(t)=&\left\{\left\{0.2\sqrt{\Gamma(t)}+\dot{\Gamma}_{\mathrm{d}}(t)-cP\big(\Gamma(t)-\Gamma_{\mathrm{d}}(t)\big)\right\}\right.\\
&\times\big(\Upsilon_{\mathrm{b}_1}-\Upsilon_{\mathrm{b}}(t)\big)-\frac{n_1\Upsilon_{\mathrm{b}}(t)\Gamma(t)}{\big(1+n_2\Upsilon_{\mathrm{b}}(t)\big)^2}-\dot{\Upsilon}_{\mathrm{bd}}(t)\Gamma(t)\\
&\left.+cP\big(\Upsilon_{\mathrm{b}}(t)-\Upsilon_{\mathrm{bd}}(t)\big)\Gamma(t)\right\}\times\frac{1}{(\Upsilon_{\mathrm{b}_1}-\Upsilon_{\mathrm{b}_2})}, \qquad (21)\\
v_2(t)=&\left\{\left\{0.2\sqrt{\Gamma(t)}+\dot{\Gamma}_{\mathrm{d}}(t)-cP\big(\Gamma(t)-\Gamma_{\mathrm{d}}(t)\big)\right\}\right.\\
&\times\big(\Upsilon_{\mathrm{b}_2}-\Upsilon_{\mathrm{b}}(t)\big)-\frac{n_1\Upsilon_{\mathrm{b}}(t)\Gamma(t)}{\big(1+n_2\Upsilon_{\mathrm{b}}(t)\big)^2}-\dot{\Upsilon}_{\mathrm{bd}}(t)\Gamma(t)\\
&\left.+cP\big(\Upsilon_{\mathrm{b}}(t)+\Upsilon_{\mathrm{bd}}(t)\big)\Gamma(t)\right\}\times\frac{1}{(\Upsilon_{\mathrm{b}_2}-\Upsilon_{\mathrm{b}_1})}. \qquad (22)
\end{aligned}$$

In this paper, (21)-(22) is called the original controller, and the proposed controller (13)-(14) is called the new controller.

IV. THEORETICAL ANALYSES ON SUPERIOR PERFORMANCE OF THE NEW CONTROLLER

The theoretical analyses of the superiority of the new controller (13)-(14) are presented in this section. Specifically, the global stability of the new controller is demonstrated. In addition, considering that there exist perturbations in the actual production of the agitator tank, theoretical analyses prove the perturbations rejection performance of the new controller.

A. CONVERGENCE ANALYSIS

In this section, the global convergence of the new controller is proved theoretically. Therefore, the following theorem is given.

Theorem 1: When $P_1(\cdot)$ and $P_2(\cdot)$ are monotonically increasing odd functions, the new controller (13)-(14) is globally stable according to the Lyapunov stability theory.

Proof: The ith subsystem of the nonlinear excitation design equation (4) can be written as follows ($\forall i\in 1,2,\ldots m$):

$$\dot{\epsilon}_i(t)=-cP_1\big(\epsilon_i(t)\big)-dP_2\left\{\epsilon_i(t)+c\int_0^t P_1\epsilon_i(\tau)\mathrm{d}\tau\right\}, \qquad (23)$$

where $\epsilon_i(t)$ represents the ith element of the error function $\epsilon(t)$. For the ith subsystem (23), define an auxiliary variable $z_i(t)$ as

$$z_i(t)=\epsilon_i(t)+c\int_0^t P_1\big(\epsilon_i(\tau)\big)\mathrm{d}\tau. \qquad (24)$$

Taking the time derivative of both sides of (24) obtains

$$\dot{z}_i(t)=\dot{\epsilon}_i(t)+cP_1\big(\epsilon_i(t)\big). \qquad (25)$$

Furthermore, combining (23), (24) and (25) gets

$$\dot{z}_i(t)=-dP_2\big(z_i(t)\big). \qquad (26)$$

Further, we design a Lyapunov function candidate $v_i(t)$ for the ith subsystem (23) as follows:

$$v_i(t)=\frac{1}{2}\sigma\epsilon_i^2(t)+\frac{1}{2}z_i^2(t), \qquad (27)$$

where $\sigma>0$ and $v_0=v_i(0)=\sigma\epsilon_i^2(0)/2+z_i^2(0)/2$. Obviously, $v_i(t)$ is positive definite. Note that $v_i(t)>0$ for any $\epsilon_i(t)\neq 0$ or $z_i(t)\neq 0$, and $v_i(t)=0$ only for $\epsilon_i(t)=z_i(t)=0$. Then the time derivative of $v_i(t)$ is derived as follows:

$$\begin{aligned}
\frac{\mathrm{d}v_i}{\mathrm{d}t}&=\sigma\epsilon_i(t)\dot{\epsilon}_i(t)+z_i(t)\dot{z}_i(t)\\
&=\sigma\epsilon_i(t)\big[\dot{z}_i(t)-cP_1\big(\epsilon_i(t)\big)\big]-dz_i(t)P_2\big(z_i(t)\big)\\
&=-\sigma d\epsilon_i(t)P_2\big(z_i(t)\big)-\sigma c\epsilon_i(t)P_1\big(\epsilon_i(t)\big)\\
&\quad-dz_i(t)P_2\big(z_i(t)\big). \qquad (28)
\end{aligned}$$

Then, we are supposed to prove $\dot{v}_i(t)\leq 0$ in what follows. Obviously, in this situation, $v_i(t)\leq v_i(0)$. Based on this, the following conclusions can be gained:

$$\frac{1}{2}\sigma\epsilon_i^2(t)\leq v_0,\ \frac{1}{2}z_i^2(t)\leq v_0. \qquad (29)$$

We can further derive

$$|\epsilon_i(t)|\leq\sqrt{2v_0/\sigma},\ \ |z_i(t)|\leq\sqrt{2v_0}. \qquad (30)$$

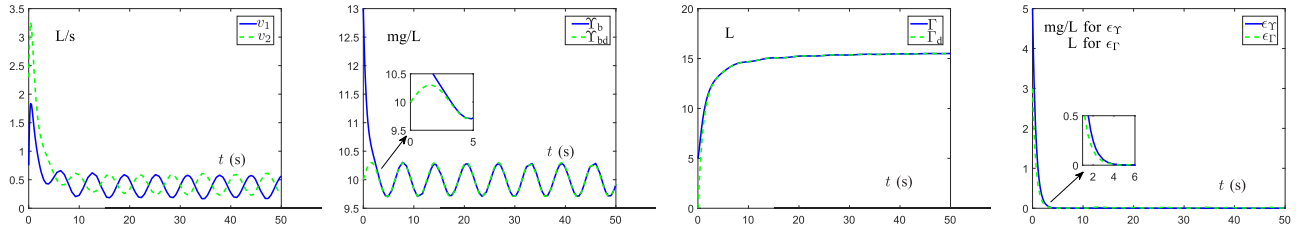

FIGURE 2. Simulation results on the production of reagents in the agitator tank equipped with the original controller (21) and (22) without perturbations. (a) Flow rates of the two input liquids in the agitator tank. (b) The concentration of the output reagent of the agitator tank. (c) The volume of the reagent in the agitator tank. (d) The output reagent concentration error (mg/L) and the liquid volume error (L) of the agitator tank.

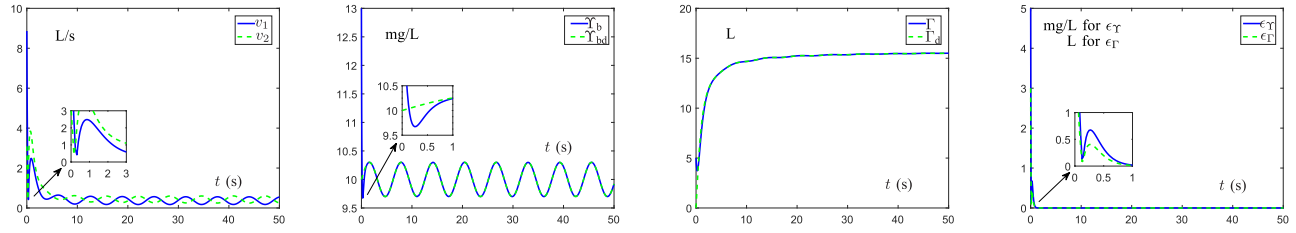

FIGURE 3. Simulation results on the production of reagents in the agitator tank equipped with the new controller (13) and (14) without perturbations. (a) Flow rates of the two input liquids in the agitator tank. (b) The concentration of the output reagent of the agitator tank. (c) The volume of the reagent in the agitator tank. (d) The output reagent concentration error (mg/L) and the liquid volume error (L) of the agitator tank.

In addition, we set X_1 and X_2 to represent $\epsilon_i(t)$ and $z_i(t)$, respectively, and obtain

$$X_1 = \left\{\epsilon_i(t) \in R, |\epsilon_i(t)| \le \sqrt{2v_0/\sigma}\right\},$$
$$X_2 = \left\{z_i(t) \in R, |z_i(t)| \le \sqrt{2v_0}\right\}. \quad (31)$$

Applying the median theorem in the bounded region X_2, we have

$$P_2\big(z_i(t)\big) - P_2(0) = \big(z_i(t) - 0\big)\frac{\partial P_2\big(z_i(\zeta)\big)}{\partial z_i}|_{z_i(\zeta)\in X_2}, \quad (32)$$

where $P_2(0) = 0$ and $\partial P_2\big(z_i(\zeta)\big)/\partial z_i > 0$. Thus, from (32), the following result can be gained:

$$\left|P_2\big(z_i(t)\big)\right| \le B_0 \left|z_i(t)\right|,$$

where $B_0 = \max\left\{\partial P_2\big(z_i(t)\big)/\partial z_i\right\}|_{z_i(t)\in X_2} > 0$ is bounded. Thus, one can have

$$\left|\epsilon_i(t)P_2\big(z_i(t)\big)\right| \le |\epsilon_i(t)| \cdot \left|P_2\big(z_i(t)\big)\right| \le B_0 |\epsilon_i(t)| \cdot |z_i(t)|. \quad (33)$$

Substituting (33) into (28), we have

$$\begin{aligned}
\frac{\mathrm{d}v_i}{\mathrm{d}t} &= -\sigma d\epsilon_i(t)P_2\big(z_i(t)\big) - \sigma c\epsilon_i(t)P_1\big(\epsilon_i(t)\big) - dz_i(t)P_2\big(z_i(t)\big) \\
&\le \sigma d\left|\epsilon_i(t)P_2\big(z_i(t)\big)\right| - \sigma c\epsilon_i(t)P_1\big(\epsilon_i(t)\big) - dz_i(t)P_2\big(z_i(t)\big) \\
&\le \sigma dB_0 |\epsilon_i(t)| \cdot |z_i(t)| - \sigma cB_1\epsilon_i^2(t) - dB_2 z_i^2(t) \\
&= -\sigma\big(\sqrt{cB_1}\,|\epsilon_i(t)| - \frac{dB_0}{2\sqrt{cB_1}}|z_i(t)|\big)^2 \\
&\quad -\sigma\big(\frac{dB_2}{\sigma} - \frac{d^2B_0^2}{4cB_1}\big)z_i^2(t),
\end{aligned}$$

where $B_1 > 0$ and $B_2 > 0$. In addition, in a similar way, $B_1 = \min\left\{\partial P_1\big(\epsilon_i(t)\big)/\partial\epsilon_i\right\}|_{z_i(t)\in X_1}$ and $B_2 = \min\left\{\partial P_2\big(z_i(t)\big)/\partial z_i\right\}|_{z_i(t)\in X_2}$ are obtained by applying the median theorem. From the above discussions, we can get $\dot{v}_i(t) \le 0$ provided that

$$0 < \sigma \le \frac{4cB_1B_2}{dB_0^2}. \quad (34)$$

The above results can guarantee the negative definite of $v_i(t)$. Therefore, according to Lyapunov stability theory, it can be concluded that the ith subsystem (23) is globally stable. In this sense, the error function $\epsilon(t)$ generated by the model (4) globally converges to zero. This proof is completed. □

B. ROBUSTNESS ANALYSIS

Conventional agitator tank controllers do not take the effects of disturbances into account, which may have a significant impact on the accuracy of preparing reagents. In this section, we add the unknown constant perturbation to the agitator system and prove that the perturbation injected model (19)-(20) is anti-disturbing.

Theorem 2: When polluted by the unknown constant perturbation, the state output of the perturbation injected model (19)-(20) globally converges to the optimal solution to equation (1)-(2) of the agitator tank system from any randomly-generated initial value.

Proof: Substitute (5)-(6) into (19)-(20), and simplify to get

$$\dot{\epsilon}(t) = -cP_1\big(\epsilon(t)\big) - dP_2\left\{\epsilon(t) + c\int_0^t P_1\big(\epsilon(\tau)\big)\mathrm{d}\tau\right\} + \Psi(t). \quad (35)$$

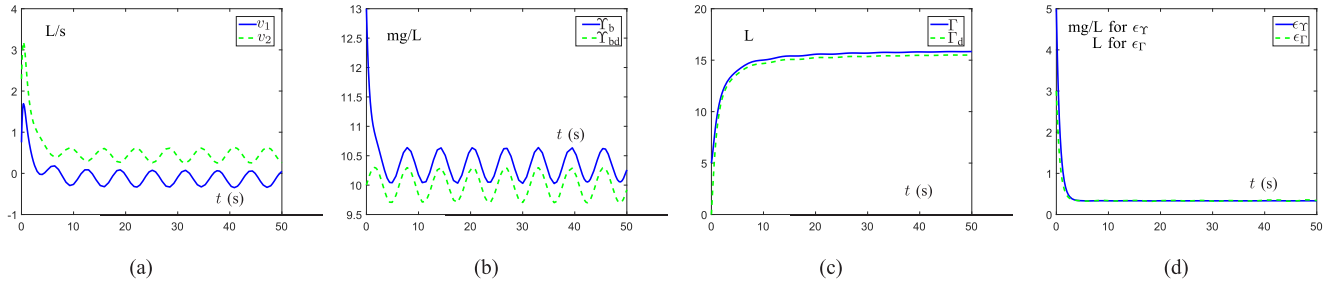

FIGURE 4. Simulation results on the production of reagents in the agitator tank equipped with the original controller with constant perturbation. (a) Flow rates of the two input liquids in the agitator tank. (b) The concentration of the output reagent of the agitator tank. (c) The volume of the reagent in the agitator tank. (d) The output reagent concentration error (mg/L) and the liquid volume error (L) of the agitator tank.

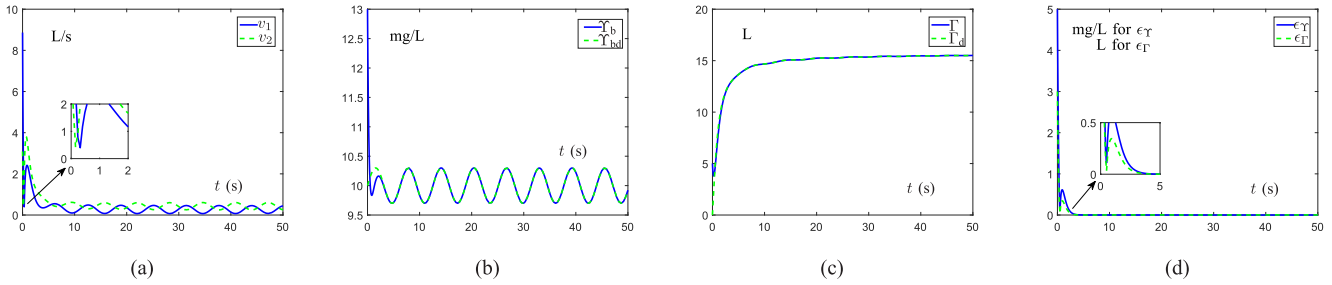

FIGURE 5. Simulation results on the production of reagents in the agitator tank equipped with the original controller with constant perturbation. (a) Flow rates of the two input liquids in the agitator tank. (b) The concentration of the output reagent of the agitator tank. (c) The volume of the reagent in the agitator tank. (d) The output reagent concentration error (mg/L) and the liquid volume error (L) of the agitator tank.

Further, the ith subsystem of the above equation can be written as

$$\dot{\epsilon}_i(t) = -cP_1\big(\epsilon_i(t)\big) - dP_2\left\{\epsilon_i(t) + c\int_0^t P_1\big(\epsilon_i(\tau)\big)\mathrm{d}\tau\right\} + \Psi(t). \quad (36)$$

We introduce the same auxiliary variable $z_i(t)$ as (24). Thus, the time derivative of $z_i(t)$ is $\dot{z}_i(t) = \dot{\epsilon}_i(t) + cP_1\big(\epsilon_i(t)\big)$. Then substituting $z_i(t)$ and $\dot{z}_i(t)$ into (36), we have

$$\dot{z}_i(t) = -dP_2\big(z_i(t)\big) + \Psi(t), \quad (37)$$

According to the above equation, the ith perturbation interference subsystem (36) selects the Lyapunov function candidate as

$$\kappa_i(t) = \big(dP_2\big(z_i(t)\big) - \Psi(t)\big)^2/2,$$

which ensures the positive definiteness of κ_i. Then, the solution of $\dot{\kappa}_i$ can be written as

$$\begin{aligned}\frac{\mathrm{d}\kappa_i}{\mathrm{d}t} &= \big(dP_2\big(z_i(t)\big) - \Psi(t)\big)d\frac{\partial P_2\big(z_i(t)\big)}{\partial z_i(t)}\dot{z}_i(t)\\ &= -d\frac{\partial P_2\big(z_i(t)\big)}{\partial z_i(t)}\big(dP_2\big(z_i(t)\big) - \Psi(t)\big)^2. \quad (38)\end{aligned}$$

Since $P_2(\cdot)$ is a monotonically increasing odd activation function, it makes $\partial P_2\big(z_i(t)\big)/\partial z_i > 0$. Therefore, we conclude that $\dot{\kappa}_i \leq 0$ and $\dot{\kappa}_i$ is negative definite, i.e., $\dot{\kappa}_i < 0$ for any $dP_2\big(z_i(t)\big) - \Psi(t) \neq 0$ and $\dot{\kappa}_i = 0$ only for $dP_2\big(z_i(t)\big) - \Psi(t) = 0$. Therefore, the Lyapunov function candidate $\kappa_i(t)$ converges to zero with time. Thus, $\lim_{t\to\infty} dP_2\big(z_i(t)\big) - \Psi(t) = 0$, i.e., $\lim_{t\to\infty} z_i(t) = P_2^{-1}(\Psi(t)/d)$. Namely, $z_i(t)$ converges to $P_2^{-1}(\Psi(t)/d)$ and $\lim_{t\to\infty}\dot{z}_i(t) = -dP_2\big(z_i(t)\big) + \Psi(t) = 0$. Considering that $\dot{z}_i(t) = \dot{\epsilon}_i(t) + cP_1\big(\epsilon_i(t)\big)$ and $\lim_{t\to\infty}\dot{z}_i(t) = 0$, we can derive that $\dot{\epsilon}_i(t) = \dot{z}_i(t) - cP_1\big(\epsilon_i(t)\big)$. When $t \to \infty$, $\dot{\epsilon}_i(t) = \dot{z}_i(t) - cP_1\big(\epsilon_i(t)\big)$ reduces to $\dot{\epsilon}_i(t) = -cP_1\big(\epsilon_i(t)\big)$. For this dynamic system, based on the results of the previous discussion, it is easy to prove that $\lim_{t\to\infty}\dot{\epsilon}_i(t) = 0$.

Based on the above analyses, when P_1 and P_2 are monotonically increasing odd activation functions, the error function $\epsilon(t)$ generated by the constant perturbation injected model (19)-(20) converges globally to zero. That is to say, starting from arbitrary initial value, the system state output of the perturbation injected model can globally converge to the optimal solution to (1)-(2), in the presence of unknown constant perturbations. The verification of the anti-perturbation ability of the proposed agitator tank controller (13)-(14) is completed. □

In summary, the above two theorems about global convergence and robustness to constant perturbations are demonstrated in detail. The superiority of the model is theoretically explained.

V. ILLUSTRATIVE EXAMPLE

In this section, we perform computer simulations on the process of preparing reagents in an agitator tank and present simulation results. Specifically, the parameters of the agitator tank are set as follows: At the initial time, the concentrations of the two input liquids are set as 24.9 mg/L and 0.1 mg/L, respectively; the inflow rates v_1 and v_2 of both liquids are set as 5 L/s; the coefficient associated with the outflow rate n_1

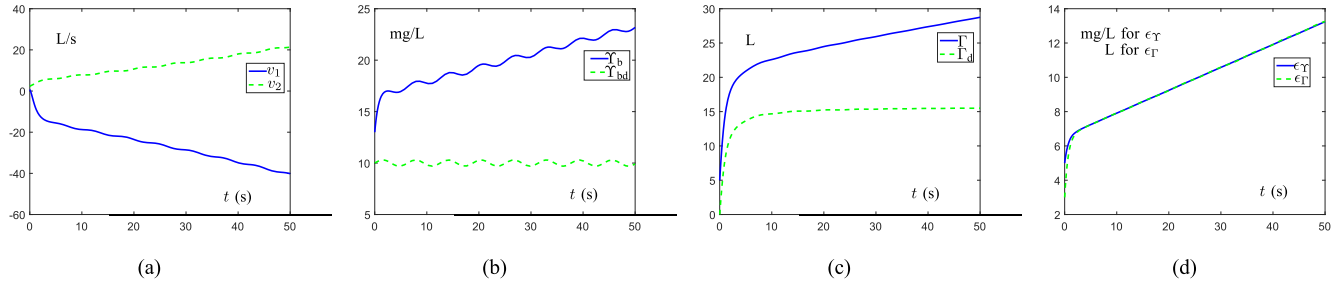

FIGURE 6. Simulation results on the production of reagents in the agitator tank equipped with the original controller with time-varying perturbation. (a) Flow rates of the two input liquids in the agitator tank. (b) The concentration of the output reagent of the agitator tank. (c) The volume of the reagent in the agitator tank. (d) The output reagent concentration error (mg/L) and the liquid volume error (L) of the agitator tank.

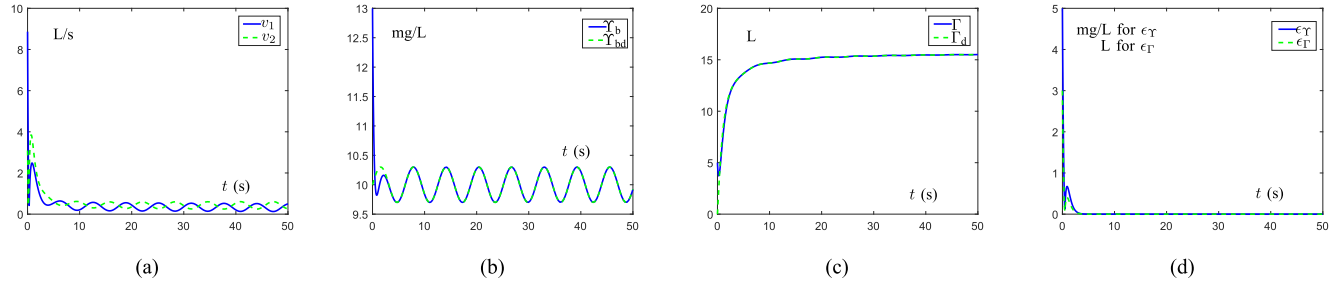

FIGURE 7. Simulation results on the production of reagents in the agitator tank equipped with the new controller with time-varying perturbation. (a) Flow rates of the two input liquids in the agitator tank. (b) The concentration of the output reagent of the agitator tank. (c) The volume of the reagent in the agitator tank. (d) The output reagent concentration error (mg/L) and the liquid volume error (L) of the agitator tank.

TABLE 1. Parameters used in article.

Parameters	Meaning	Value
Υ_1, Υ_2	Influent liquid concentration	24.9, 0.1
Υ_b	Effluent liquid concentration	**No**
Υ_{bd}	Desired effluent liquid concentration	10
Γ	Actual solution volume	**No**
Γ_d	Desired solution volume	15
v_1, v_2	Inflow rate	5, 5
c, d	Convergence rate	1.5, 1.5
n_1, n_2	Coefficient	1, 1
$P_1(\cdot), P_2(\cdot)$	Monotonically increasing odd function	$(\cdot)^3, (\cdot)^3$

No stands for no fixed value.

and n_2 are set as 1; parameters c and d are both set as 1.5; the desired solution volume Γ_d in the agitator tank is 15 L; the desired solution concentration Υ_{bd} in the agitator tank is 10 mg/L; the monotonically increasing odd functions $P_1(\cdot) = P_2(\cdot) = (\cdot)^3$; the computer simulation time is designed as 50 s. Simulation experiments synthesized by the original controller (21)-(22) and the new controller (13)-(14) for the agitator tank preparing reagents are conducted to demonstrate the high performance of the new controller. For convenient reading, the parameters used in simulations are arranged in Table 1.

A. SIMULATIONS WITHOUT PERTURBATION

In the absence of disturbances, simulation results of the agitator tank preparing reagents with the aid of the original controller (21)-(22) are given in Fig. 2. For comparison, the simulation results on the agitator tank preparing reagents with the aid of the new controller (13)-(14) are depicted in Fig. 3. Observing Fig. 2(a) with Fig. 3(a), it can be seen that the original controller and the new controller can effectively control the flow rates v_1 and v_2 of the input liquid of the agitating tank. As Fig. 2(b) demonstrates, the concentration of the output reagent of the agitator tank reaches the desired one at approximate 4 s. For comparison, in Fig. 3(b), the concentration of the output reagent from the agitator tank reaches the desired one at approximate 1 s. Comparing Fig. 2(c) and Fig. 3(c), the volume of the solution in the agitator tank reaches the desired value at 15 s for the two controllers. In addition, the output reagent concentration error and the volume error of the agitator tank converge to zero at about 4 s as shown in Fig. 2(d). However, Fig. 3(d) shows that the output reagent concentration error and volume error of the agitator tank converge to zero at approximate 1 s. Particularly, in the absence of perturbations, the error of the reagent produced by the agitator tank equipped with the new controller converges to zero for 3 s less than that of the original controller, which is a threefold increase in productivity. The above analyses verify that the new controller proposed in this paper has better convergence performance compared with the original controller.

B. SIMULATIONS UNDER CONSTANT PERTURBATION

In this subsection, we add a constant perturbation to the agitator tank system to verify the robustness of the new controller (13)-(14). For further explanation, the constant perturbation in the numerical simulations is set as 0.5. The corresponding simulations are conducted with simulation results presented in Fig. 4 and Fig. 5. Simulation results of the agitator

TABLE 2. Comparisons among different controllers for the industrial agitator tank.

	Convergent time without perturbation	Convergent time with perturbations	Constant perturbation rejection	Non-constant perturbation rejection
New controller	1 s	2.5 s	Yes*	Yes*
Original controller	4 s	$+\infty$	No⋆	No⋆

$*$ represents that the controller can reject perturbations with convergence theoretically guaranteed.
$\star$ stands for that the controller does not specifically consider perturbations rejection.

tank preparing reagents equipped with the original controller (21)-(22) are shown in Fig. 4. As a contrast, simulation results on the agitator tank preparing reagents equipped with the new controller proposed in this paper are provided in Fig. 5. As is vividly depicted in Fig. 4(a), the simulation result shows that the original controller cannot effectively control the flow rates v_1 and v_2 of the input agitator tank. In addition, Fig. 4(b) shows that there exists a large error between the actual output reagent concentration and the desired output. It is noteworthy that the volume of the solution in Fig. 4(c) in the agitator tank also deviates from the desired value. Fig. 4(d) demonstrates that the error between the concentration of the output reagent and the desired concentration, and the error between the volume of the solution in the agitator tank and the desired volume, which are not convergent to zero. In brief, the original controller has poor performance when polluted by perturbations. Moreover, it is readily discovered that the new controller can effectively control the flow rate of the input liquid to the agitator tank in Fig. 5(a). Additionally, Fig. 5(b) and (c) indicate that both the output reagent concentration of the agitator tank equipped with the new controller and the volume of the solution in the tank can reach the desired values. As can be observed in Fig. 5(d), when the agitator tank system is disturbed by constant perturbations, the output reagent concentration error and the volume error of the agitator tank can converge to zero within about 5 s. Through all the above simulation experiments, we come to the conclusion that the new controller has the perturbation rejection performance compared with the original controller under the constant perturbation.

C. SIMULATIONS UNDER NON-CONSTANT PERTURBATION

The agitator tank may be subjected to non-constant perturbations in actual operation. In response to this situation, the numerical simulations of the agitator tank with the non-constant perturbation are conducted. Specifically, the simulation results of the agitator tank equipped with the original controller (21)-(22) and the new controller (13)-(14) are shown in Fig. 6 and Fig. 7, respectively. It is worth noting that time-varying perturbations are common in industrial production and can increase over time. Therefore, in the simulations, the time-varying perturbation $0.1t + 10$ is added to the agitator tank system. It can be seen from Fig. 6(a) that the original agitator tank cannot stably control the flow rate of the input liquid. Furthermore, Fig. 6(b) illustrates that the concentration of the solution produced by the agitator tank equipped with the original controller deviates from the desired value, and the deviation increases as time evolves. Moreover, it is observed in Fig. 6(c) that the actual solution volume in the agitator tank exceeds the desired value. Finally, Fig. 6(d) illustrates that the concentration error and volume error of the solution prepared in the agitator tank cannot converge to zero. Thereafter, it can be viewed from Fig. 7(a) that the agitator tank equipped with the new controller can normally control the flow rate of the input liquid. In addition, by observing Fig. 7(b) and (c), it is found that the concentration and volume of the reagent prepared in the agitator tank are almost the same as the desired values after 2.5 s. Lastly, Fig. 7(d) describes the error convergence effect of the prepared reagent parameters. Concretely, the concentration error and volume error of the solution both converge to near zero. In summary, the simulation experiments verify that the proposed controller has perturbations rejection performance under the non-constant perturbation compared to the original controller.

VI. CONCLUSION

In this paper, a new neural dynamic agitator tank controller has been presented. Compared with the original controller theoretical analysis shows that the new controller has fast convergence performance and strong robustness. In addition, in order to further verify these performances of the new controller, we have executed the computer simulations on the agitator tank formulation reagents. Simulation results have indicated that the agitator tank synthesized by the proposed controller has an excellent performance compared with the original controller. Specifically, the reagent concentration and solution volume of the agitator tank equipped with the proposed controller are able to quickly converge to the desired values. In addition, when polluted by noises, the agitator tank equipped with the new controller can still prepare the target reagents with high performance. These superior properties can reduce the waste of industrial materials and greatly increase production efficiency.

REFERENCES

[1] A. S. McKim, "Overcoming sustainability barriers within the chemical industry," *Current Opinion Green Sustain. Chem.*, vol. 14, no. 5, pp. 10–13, 2018.
[2] S. F. Banda and K. Sichilongo, "Analysis of the level of comprehension of chemical hazard labels: A case for Zambia," *Sci. Total Environ.*, vol. 363, nos. 1–3, pp. 22–27, 2006.

[3] S. M. Zala and D. J. Penn, "Abnormal behaviours induced by chemical pollution: A review of the evidence and new challenges," *Animal Behav.*, vol. 68, no. 5, pp. 649–664, 2004.

[4] F. W. Lichtenthaler and S. Peters, "Carbohydrates as green raw materials for the chemical industry," *Pattern Recognit.*, vol. 7, no. 4, pp. 65–90, 2004.

[5] E. Andersson, M. Karlsson, S. Paramonova, and P. Thollander, "Energy end-use and efficiency potentials among Swedish industrial small and medium-sized enterprises—A dataset analysis from the national energy audit program," *Renew. Sustain. Energy Rev.*, vol. 93, no. 2, pp. 165–177, 2018.

[6] A. M. Bessarabov, A. V. Avseev, V. V. Avseev, and A. M. Kutepov, "Information technologies in the industry of chemical reagents and special-purity substances," *Theor. Found. Chem. Eng.*, vol. 38, no. 1, pp. 214–218, 2004.

[7] T. Edwiges, L. Frare, B. Mayer, L. Lins, J. M. Triolo, X. Flotats, and M. S. S. M. Costa, "Influence of chemical composition on biochemical methane potential of fruit and vegetable waste," *Waste Manage.*, vol. 71, no. 4, pp. 618–625, 2018.

[8] T. Jackson, "Clean production strategies: Developing preventive environmental management in the industrial economy," *Ecol. Econ.*, vol. 12, no. 4, pp. 84–85, 1993.

[9] S. G. Newman and K. F. Jensen, "The role of flow in green chemistry and engineering," *Green Chem.*, vol. 15, no. 4, pp. 1456–1472, 2013.

[10] M. J. Pearse, "An overview of the use of chemical reagents in mineral processing," *Minerals Eng.*, vol. 18, no. 10, pp. 139–149, 2005.

[11] R. Shamsoddini and N. Aminizadeh, "Incompressible smoothed particle hydrodynamics modeling and investigation of fluid mixing in a rectangular stirred tank with free surface," in *Chem. Eng. Commun.*, vol. 204, no. 5, pp. 563–572, 2017.

[12] R. D. Biggs, "Mixing rates in stirred tanks," *AIChE J.*, vol. 9, no. 5, pp. 636–640, 1963.

[13] K R. Rao and J. B. Joshi, "Liquid phase mixing in mechanically agitated vessels," *Chem. Eng. Commun.*, vol. 74, no. 2, pp. 1–25, 1988.

[14] J. Min and Z. Gao, "Large eddy simulations of mixing time in a stirred tank," *Chin. J. Chem. Eng.*, vol. 14, no. 99, pp. 1–7, 2006.

[15] R. Zadghaffari, J. S. Moghaddas, and J. Revstedt, "A mixing study in a double-Rushton stirred tank," *Comput. Chem. Eng.*, vol. 33, no. 3, pp. 1240–1246, 2009.

[16] M. Martín, F. J. Montes, and M. A. Galán, "Bubbling process in stirred tank reactors I: Agitator effect on bubble size, formation and rising," *Chem. Eng. Sci.*, vol. 63, no. 1, pp. 3212–3222, 2008.

[17] M. H. Xie, G. Z. Zhou, S. Meng, B. Wang, and S. L. Du, "Numerical simulation of flow property in polymer dissolution tank with inner-outer agitators," *Chem. Eng. J.*, vol. 40, no. 3, pp. 10–11, 2012.

[18] Y. Arima and A. Hirose, "Performance dependence on system parameters in millimeter-wave active imaging based on complex-valued neural networks to classify complex texture," *IEEE Access*, vol. 5, pp. 22927–22939, 2017.

[19] J.-P. Cai, L. Xing, M. Zhang, and L. Shen, "Adaptive neural network control for missile systems with unknown hysteresis input," *IEEE Access*, vol. 5, pp. 15839–15847, 2017.

[20] Y. Shen and J. Wang, "Robustness analysis of global exponential stability of recurrent neural networks in the presence of time delays and random disturbances," *IEEE Trans. Neural Netw. Learn. Syst.*, vol. 23, no. 1, pp. 87–96, Jan. 2012.

[21] Y. Zhang, S. Li, and L. Liao, "Consensus of high-order discrete-time multiagent systems with switching topology," *IEEE Trans. Syst., Man, Cybern., Syst.*, to be published. doi: 10.1109/TSMC.2018.2882558.

[22] Y. Zhang, S. Li, J. Zou, and A. H. Khan, "A passivity-based approach for kinematic control of redundant manipulators with constraints," *IEEE Trans. Ind. Informat.*, to be published. doi: 10.1109/TII.2019.2908442.

[23] Y. Zhang, S. Li, S. Kadry, and B. Liao, "Recurrent neural network for kinematic control of redundant manipulators with periodic input disturbance and physical constraints," *IEEE Trans. Cybern.*, to be published. doi: 10.1109/TCYB.2018.2859751.

[24] Y. Zhang, S. Li, and X. Zhou, "Recurrent-neural-network-based velocity-level redundancy resolution for manipulators subject to a joint acceleration limit," *IEEE Trans. Ind. Electron.*, vol. 66, no. 5, pp. 3573–3582, May 2019.

[25] Y. Zhang, S. Li, and L. Liao, "Near-optimal control of nonlinear dynamical systems: A brief survey," *Annu. Rev. Control*, vol. 47, pp. 71–80, 2019. doi: 10.1016/j.arcontrol.2019.01.003.

[26] M. Tan, "Asymptotic stability of nonlinear systems with unbounded delays," *J. Math. Anal. Appl.*, vol. 37, no. 2, pp. 1010–1021, 2008.

[27] L. Xiao and R. Lu, "Finite-time solution to nonlinear equation using recurrent neural dynamics with a specially-constructed activation function," *Neurocomputing*, vol. 151, no. 3, pp. 246–251, Mar. 2015.

[28] W. Duan, L. Jin, B. Hu, H. Lu, M. Liu, K. Li, L. Xiao, and C. Yi, "Nonlinearity activated noise-tolerant zeroing neural network for real-time varying matrix inversion," in *Proc. 37th Chin. Control Conf.*, 2018, pp. 3117–3122.

[29] L. Jin and S. Li, "Distributed task allocation of multiple robots: A control perspective," *IEEE Trans. Syst., Man, Cybern. Syst.*, vol. 48, no. 5, pp. 693–701, May 2018.

[30] L. Jin, Y. Zhang, and S. Li, "Integration-enhanced Zhang neural network for real-time-varying matrix inversion in the presence of various kinds of noises," *IEEE Trans. Neural Netw. Learn. Syst.*, vol. 27, no. 4, pp. 2615–2627, Dec. 2016.

[31] L. Jin, Y. Zhang, S. Li, and Y. Zhang, "Noise-tolerant ZNN models for solving time-varying zero-finding problems: A control-theoretic approach," *IEEE Trans. Autom. Control*, vol. 62, no. 2, pp. 992–997, Feb. 2017.

[32] D. Zhao, W. Chen, J. Wu, and J. Li, "Globally stable adaptive tracking control for uncertain strict-feedback systems based on neural network approximation," *Asian J. Control*, vol. 18, no. 10, pp. 527–538, 2016.

[33] J. Cai and X. Li, "Dry mortar mixing storage control system based on the BP neural PID," *Manuf. Automat.*, vol. 3, no. 5, pp. 31–33, 2012.

[34] Y. Zhang, Y. Ding, B. Qiu, J. Wen, and X. Li, "ZD method based nonlinear and robust control of agitator tank," *Asian J. Control*, vol. 20, no. 4, pp. 1464–1479, 2018.

[35] K. Zhang, M. Staroswiecki, and B. Jiang, "Static output feedback based fault accommodation design for continuous-time dynamic systems," *Int. J. Control*, vol. 84, no. 3, pp. 412–423, 2011.

[36] Y. Zhang, B. Mu, and H. Zheng, "Link between and comparison and combination of Zhang neural network and quasi-Newton BFGS method for time-varying quadratic minimization," *IEEE Trans. Cybern.*, vol. 43, no. 2, pp. 490–503, Apr. 2013.

[37] A. Bessarabov and A. Afanas'ev, "CALS technologies in design of promising chemical production units," *Khim. Tekhnol.*, vol. 3, no. 1, p. 26, 2002.

[38] L. Jin, Y. Zhang, T. Qiao, M. Tan, and Y. Zhang, "Tracking control of modified Lorenz nonlinear system using ZG neural dynamics with additive input or mixed inputs," *Neurocomputing*, vol. 196, no. 4, pp. 82–94, 2016.

[39] X. Zhang and G. Ahmadi, "Eulerian–Lagrangian simulations of liquid–gas–solid flows in three-phase slurry reactors," *Chem. Eng. Sci.*, vol. 60, no. 6, pp. 5089–5104, 2005.

[40] L. Li and B. Xu, "Accurate tracking control of linear synchronous motor machine tool axes," *Chin. J. Mech. Eng.*, vol. 30, no. 4, pp. 118–126, 2017.

[41] G. Li and Y. Lin, "Adaptive output feedback control for a class of nonlinear systems with quantised input and output," *Int. J. Control*, vol. 90, no. 12, pp. 239–248, 2017.

[42] Z. Xie, L. Jin, X. Du, X. Xiao, H. Li, and S. Li, "On generalized RMP scheme for redundant robot manipulators aided with dynamic neural networks and nonconvex bound constraints," *IEEE Trans. Ind. Informat.*, to be published. doi: 10.1109/TII.2019.2899909.

[43] A. W. Nienow, "Stirring and stirred-tank reactors," *Chem. Ingenieur Technik*, vol. 8, no. 4, pp. 2063–2074, 2014.

[44] H. Lu, L. Jin, X. Luo, B. Liao, D. Guo, and L. Xiao, "RNN for solving perturbed time-varying underdetermined linear system with double bound limits on residual errors and state variables," *IEEE Trans. Ind. Informat.*, to be published. doi: 10.1109/TII.2019.2909142.

[45] Y. Zhang, W. Ma, and B. Cai, "From Zhang neural network to Newton iteration for matrix inversion," *IEEE Trans. Circuits Syst. I, Reg. Papers*, vol. 56, no. 7, pp. 1405–1415, Jul. 2009.

[46] Y. Zhang and S. S. Ge, "Design and analysis of a general recurrent neural network model for time-varying matrix inversion," *IEEE Trans. Neural Netw.*, vol. 16, no. 6, pp. 1477–1490, Nov. 2005.

[47] L. Wei, L. Jin, C. Yang, K. Chen, and W. Li, "New noise-tolerant neural algorithms for future dynamic nonlinear optimization with estimation on hessian matrix inversion," *IEEE Trans. Syst., Man, Cybern., Syst.*, to be published. doi: 10.1109/TSMC.2019.2916892.

[48] L. Xiao, S. Li, J. Yang, and Z. Zhang, "A new recurrent neural network with noise-tolerance and finite-time convergence for dynamic quadratic minimization," *Neurocomputing*, vol. 285, pp. 125–132, Apr. 2018.

[49] Z. Zhang, T. Fu, Z. Yan, L. Jin, L. Xiao, Y. Sun, Z. Yu, and Y. Li, "A varying-parameter convergent-differential neural network for solving joint-angular-drift problems of redundant robot manipulators," *IEEE/ASME Trans. Mechatronics*, vol. 23, no. 2, pp. 679–689, Apr. 2018.

[50] L. Jin, S. Li, H. M. La, and X. Luo, "Manipulability optimization of redundant manipulators using dynamic neural networks," *IEEE Trans. Ind. Electron.*, vol. 64, no. 6, pp. 4710–4720, Jun. 2017.
[51] L. Ding, L. Xiao, K. Zhou, Y. Lan, and Y. Zhang, "A new RNN model with a modified nonlinear activation function applied to complex-valued linear equations," *IEEE Access*, vol. 6, pp. 62954–62962, 2018.
[52] L. Jin, S. Li, X. Luo, and Y. Li, "Neural dynamics for cooperative control of redundant robot manipulators," *IEEE Trans. Ind. Informat.*, vol. 14, no. 9, pp. 3812–3821, Sep. 2018.
[53] L. Jin, S. Li, B. Hu, M. Liu, and J. Yu, "A noise-suppressing neural algorithm for solving the time-varying system of linear equations: A control-based approach," *IEEE Trans. Ind. Informat.*, vol. 15, no. 1, pp. 236–246, Jan. 2019.

WENHUI DUAN received the B.E. degree from Jinzhong University, Shanxi, China, in 2017. He is currently pursuing the M.E. degree in electronics and communication engineering with the School of Information Science and Engineering, Lanzhou University, Lanzhou, China. His research interests include neural networks and robotics.

XIUCHUN XIAO received the Ph.D. degree in communication and information system from Sun Yat-sen University, Guangzhou, China, in 2013. He is currently an Associate Professor with Guangdong Ocean University. His current research interests include artificial neural networks and computer vision.

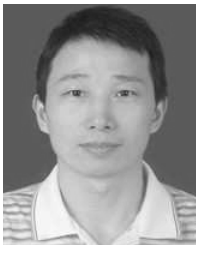

DONGYANG FU received the Ph.D. degree from the South China Sea Institute of Oceanology, Chinese Academy of Sciences, and the Ph.D. degree from the State Key Laboratory of Satellite Ocean Environment Dynamics, Second Institute of Oceanography, State Oceanic Administration, Guangzhou, China. He is currently a Professor with the School of Electronics and Information Engineering, Guangdong Ocean University, Zhanjiang, China. His current research interests include ocean color remote sensing and its application, remote sensing in offshore water quality, response of upper ocean to typhoon, and neural networks.

JINGWEN YAN received the Ph.D. degree in optics from the State Key Laboratory of Applied Optics, Changchun Institute of Fine Mechanics and Optics, Academia Sinica, in 1997. He is currently a Professor with the Department of Electronic Engineering, Shantou University, China. He is also the Associate Director of the Key laboratory of Digital Signal and Image Processing of Guangdong Province, China. Since September 2006, he has been with the Department of Electronic Engineering, Shantou University. His current research interests include SAR image processing, hyper-wavelet transforms, and compressed sensing.

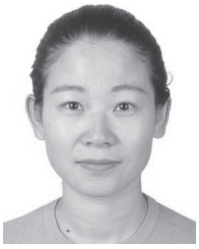

MEI LIU received the B.E. degree in communication engineering from Yantai University, Yantai, China, in 2011, and the M.E. degree in pattern recognition and intelligent system from Sun Yat-sen University, Guangzhou, China, in 2014. She is currently a Teacher with the School of Information Science and Engineering, Lanzhou University, Lanzhou, China. Before joining Lanzhou University, in 2017, she was a Lecturer with the College of Physics, Mechanical and Electrical Engineering, Jishou University, Jishou, China. Her main research interests include neural networks, computation, and optimization.

JILIANG ZHANG (M'15) received the B.S., M.S., and Ph.D. degrees from the Harbin Institute of Technology, in 2007, 2009, and 2014, respectively. He is currently an Associate Professor with the School of Information Science and Engineering, Lanzhou University, China. His research interests include neural networks, MIMO channel measurement and modeling, single radio frequency MIMO systems, relay systems, and wireless ranging systems.

LONG JIN (M'17) received the B.E. degree in automation and the Ph.D. degree in information and communication engineering from Sun Yat-sen University, Guangzhou, China, in 2011 and 2016, respectively. He is currently a Full Professor with the School of Information Science and Engineering, Lanzhou University, Lanzhou, China. Before joining Lanzhou University, in 2017, he was a Postdoctoral Fellow with the Department of Computing, The Hong Kong Polytechnic University, Hong Kong. His main research interests include neural networks, robotics, and intelligent information processing.